IEEE Access
Multidisciplinary | Rapid Review | Open Access Journal

Received December 7, 2020, accepted January 2, 2021, date of publication January 5, 2021, date of current version January 20, 2021.

Digital Object Identifier 10.1109/ACCESS.2021.3049280

A Short-Term Optimal Scheduling Model for Wind-Solar-Hydro Hybrid Generation System With Cascade Hydropower Considering Regulation Reserve and Spinning Reserve Requirements

JUN XIE[1], (Member, IEEE), YIMIN ZHENG[1], XUEPING PAN[1], (Member, IEEE), YUAN ZHENG[1], LIQIN ZHANG[1], AND YONGSHENG ZHAN[2]

[1]College of Energy and Electrical Engineering, Hohai University, Nanjing 210098, China
[2]Yalong River Hydropower Development Company Ltd., Chengdu 610051, China

Corresponding author: Jun Xie (jxie@hhu.edu.cn)

This work was supported in part by the National Natural Science Foundation of China under Grant U1965104, and in part by the National Key Research and Development Program of China under Grant 2019YFE0105200.

ABSTRACT In order to meet the challenges brought by the high penetration of intermittent and fluctuating wind and solar power, a short-term optimal scheduling model for wind-solar-hydro hybrid generation system with cascade hydropower is established with the objective of minimizing the amount of abandoned wind, solar and hydro power and maximizing the stored energy of hydro stations. Cascade hydropower is considered to provide spinning reserve and regulation reserve to ensure the security of system. Mixed Integer Linear Programming (MILP) method is used for the short-term optimal schedule of wind-solar-hydro hybrid generation system. The case studies show that spinning reserve and regulation reserve are beneficial to the hybrid generation system, and verify the practical applicability of the proposed model.

INDEX TERMS Wind-solar-hydro hybrid generation system, spinning reserve, regulation reserve, MILP.

NOMENCLATURE

A. SETS

NT, t	Set and index of time periods
T	Index of the terminal time period
ND, d	Set and index of loads
NW, w	Set and index of wind farms
NV, v	Set and index of solar power stations
NH, h	Set and index of hydro stations
NL, l	Set and index of transmission lines
U_h, j	Set and index of upstream hydro stations of station h.
E_h, r	Set and index of downstream hydro stations of station h

B. PARAMETERS

Δt	Time duration
V_h^{ini}	Initial water volume of hydro station h
$V_{h,\min}$	Minimum water volume of hydro station h
$V_{h,\max}$	Maximum water volume f hydro station h
θ_h	Conversion rate of hydro station h
$P_{w,\max}$	Generation capability of wind farm w
$P_{v,\max}$	Generation capability of solar power station v
nq_h	Natural inflow of hydro station h
$P_{h,\min}$	Minimum output of hydro station h
$P_{h,\max}$	Maximum output of hydro station h
$qH_{h,\min}$	Minimum discharge volume of hydro station h
$qH_{h,\max}$	Maximum discharge volume of hydro station h
Λ	Time for water released from the upstream hydro station to the downstream hydro station
η_h	Conversion coefficient of hydro station h
$PL_{d,t}$	System load d at time t
TL_l	Transmission power limit on line l
D	Power transmission distribution matrix
Ru_h	Ramp-up capability of hydro station h
Rd_h	Ramp-down capability of hydro station h
α	Degree of wind power fluctuation
β	Degree of solar power fluctuation
$US_{h,\max}$	Maximum up spinning reserve contribution of hydro station h

The associate editor coordinating the review of this manuscript and approving it for publication was Elizete Maria Lourenco.

$DS_{h,\max}$	Maximum down spinning reserve contribution of hydro station h
τ_u	Coefficient of maximum up spinning reserve
τ_d	Coefficient of maximum down spinning reserve
$\lambda^{\pm}$	Coefficients of up (or down) spinning reserve requirement for wind power
$\mu^{\pm}$	Coefficients of up (or down) spinning reserve requirement for solar power

C. VARIABLES

$P_{w,t}$	Power output of wind farm w at time t
$P_{v,t}$	Power output of solar power station v at time t
$P_{h,t}$	Power output of hydro station h at time t
$I_{h,t}$	On/off status of hydro station h at time t
$qH_{h,t}$	Water consumption of hydro station h at time t
$h_{h,t}$	Water head of hydro station h at time t
$QI_{h,t}$	Water spillage of hydro station h at time t
$V_{h,t}$	Water volume of hydro station h at time t
$US_{h,t}$	Up spinning reserve contribution of hydro station h at time t
$DS_{h,t}$	Down spinning reserve contribution of hydro station h at time t
$AW_{w,t}$	Abandoned wind power of wind farm w at time t
$AV_{v,t}$	Abandoned solar power of solar station v at time t

I. INTRODUCTION

With more and more concern on energy shortage and global environmental degradation, constructing sustainable energy systems have become a tendency for power system nowadays [1]. Solar and wind energy, as green generation sources, are gaining acceptance for meeting energy demand at low cost without any harmful emissions [2]. However, owing to being greatly influenced by meteorological and environmental factors, solar and wind power have intermittency, strong volatility and poor controllability [3], [4]. There have been serious problems in the scheduling of wind and solar energy generation system, especially in system operation and ancillary services [5], [6].

On the contrary, hydropower has various advantages for power system operations, such as good controllability, short initiating time, and ability of storing energy. Wind, solar and hydro are complementary in time and space [7]. The introduction of hydropower can enhance the flexibility and adjustability of complementary generation systems, which can also increase the overall utilization level of renewable energy [8], [9]. An *et al.* [10] establish a coordinated optimization model with the minimum output volatility, and compare scheduling schemes of a multi-energy power system in three different weather conditions in Qinghai Province. Results show that the coordinated operation could stabilize the volatility of wind and solar power. Matevosyan *et al.* [11] put forward a method of the day-ahead operation of hydro-wind power system considering the uncertain power outputs of wind farms. Results indicate that their coordinated operation is conducive to the minimization of wind power curtailment. Apostolopoulou and McCulloch *et al.* [12] propose an optimal dispatch scheme for a hydroelectric system coupled with solar generation, and the simulation results verify the coupling of hydropower and solar power is beneficial due to the negative correlation of rain and sunshine. Shen *et al.* [13] presents a methodology for hydrothermal system generation scheduling considering multiple provincial peak-shaving demands. Zhang *et al.* [14] coordinate optimal operation of hydro–wind–solar integrated systems by modelling the uncertainties of wind and solar power represented through the generation of typical scenarios. It is a development trend to construct wind-solar-hydro hybrid generation systems, which utilize the characteristics of continuous, adjustable and controllable output of hydropower to compensate for the random fluctuation and variation of wind and solar power generation.

However, with the increasing penetration of wind power and solar power generation, reasonable reserve arrangement is facing severe challenges. With the development of wind power and solar power generation technology, many scholars have studied the modeling of wind power and photovoltaic power. Hagspiel *et al.* [15], [16] generate multivariate wind speed distributions and solar irradiance data by using a copula. Yang *et al.* [17] use time-forward kriging to forecast solar irradiance at unobserved locations. The incorporation of wind and solar power should be considered in the short-term scheduling problem, and arrange appropriate spinning reserve to maintain an adequate level of supply reliability and respond to the system load pickup after accidents.

Chen [18] points out that, in addition to the up-spinning reserve, enough down spinning reserve should be employed to satisfy the sudden rise of wind power generation at low system load times, therefore to avoid the forced shutdown of traditional units. Germán *et al.* [19] arrange thermal power units to provide both up and down spinning reserve to guarantee the committed generation resources will be able to cope with any wind power generation output realized within range. In terms of the scheduling of hybrid generation system with hydropower, Liu *et al.* [20] use hydropower to compensate for wind and solar power forecast errors to avoid power shortages. Li *et al.* [21] present a day-ahead coordinated scheduling method of hydro and wind power generation systems with consideration of uncertainties. Peng *et al.* [22] establish a flexible robust optimization with adjustable uncertainty budget dispatch model for hybrid generation system. Shen *et al.* [23] employ additional positive reserve and negative reserve to handle the forecast errors of wind and solar power. Zhong *et al.* [24] present a short-term scheduling methodology for cascaded hydro systems considering the provision of reserve services.

It is noteworthy that instead of thermal power, [20]–[24] choose hydropower to provide up and down spinning reserve which is more environment-friendly, has better ramping capability and energy storage possibility in form of hydro reservoirs. Nevertheless, to the best knowledge of the authors, the present research have not noticed that high wind and

solar penetrations can also aggravate the system frequency security. Cascade hydropower systems are desirable candidates to deal with the problem of frequency problem caused by wind and solar power fluctuations by providing regulation reserve for the hybrid generation system since they have excellent regulation performances. Therefore, how to coordinate the configuration of spinning reserve and regulation reserve provided by cascade hydropower in wind-solar-hydro hybrid generation system remains to be studied.

In this paper, we establish a short-term optimal scheduling model for wind-solar-hydro hybrid generation system with cascade hydropower. The objective is to conserve resources, i.e., reduce the forced abandoned energy and store the remaining energy as much as possible under the conditions of meeting the load demand and ensuring the safe and stable operation of the hybrid system. The main contributions of this paper are as follows:

(i) Taking the minimum of abandoned wind, solar and hydro power and the maximum of energy storage of cascade hydropower as the objectives, considering the spinning reserve and regulation reserve provided by hydropower for accommodating the intermittence and fluctuation of wind power and solar power, a short-term optimal scheduling model for wind-solar-hydro hybrid generation system with cascade hydropower is proposed.

(ii) The non-linear objective functions and constraints in the optimal scheduling model for wind-solar-hydro hybrid generation system with cascade hydropower are transformed into a mixed integer linear model by linearization and solved by CPLEX solver. The numerical studies of two cases verify the effectiveness of the proposed model.

The remainder of this paper is organized as follows. In Section 2, we present the model in detail, including objective functions and complex constraints. The spinning reserve and regulation reserve provided by hydropower are modelled in this section. In Section 3, we illustrate the proposed model through two case studies and discuss why spinning reserve and regulation reserve are beneficial for the hybrid generation system. In Section 4, we make concluding remarks and discuss on future work.

II. SHORT TERM SCHEDULING MODEL FOR WIND-SOLAR-HYDRO HYBRID GENERATION SYSTEM

In the optimal scheduling model of wind-solar-hydro hybrid power generation system with cascade hydropower, the objectives generally include the highest utilization rate of clean energy and the lowest generating cost, and the constraints generally include wind power output constraints, solar power output constraints, cascade hydropower constraints and the system constraints for regulation reserve and spinning reserve. In particular, the cascade hydropower stations have complex power and hydraulic connections. Therefore, the optimal scheduling model belongs to a multi-variable, multi-period and nonlinear optimization problem.

A. OBJECTIVE FUNCTION

In order to reduce the abandoned wind, solar and hydro power. The objective function can be expressed as follows:

$$\min \sum_{t=1}^{NT} \left(\sum_{w=1}^{NW} AW_{w,t} + \sum_{v=1}^{NV} AV_{v,t} + \sum_{h=1}^{NH} \left(QI_{h,t} \cdot \theta_h \right) \right) \cdot \Delta t \tag{1}$$

In order to store as much water as possible to meet the needs of power generation and water consumption in the future. The objective function can be expressed as follows:

$$\max \sum_{h=1}^{NH} \left[\left(V_{h,T} - V_h^{ini} \right) \cdot \sum_{r \in E_h} \theta_r \right] \tag{2}$$

The dimensions of the abandoned wind, solar and hydro energy, as well as the stored hydro energy in cascade hydropower stations, are the same, i.e., MWh. Therefore, the above objective functions can be transformed into a single objective function with equal weight, which is expressed as:

$$\min \sum_{t=1}^{NT} \left(\sum_{w=1}^{NW} AW_{w,t} + \sum_{v=1}^{NV} AV_{v,t} + \sum_{h=1}^{NH} \left(QI_{h,t} \cdot \theta_h \right) \right) \cdot \Delta t - \sum_{h=1}^{NH} \left[\left(V_{h,T} - V_h^{ini} \right) \cdot \sum_{r \in E_h} \theta_r \right] \tag{3}$$

B. CONSTRAINTS

Constraints include wind power constraints, solar power constraints, cascade hydropower constraints and system constraints:

1) WIND POWER CONSTRAINTS

Limited by the physical characteristics of wind turbines and wind energy resources, the constraints on the wind power output are expressed as:

$$0 \le P_{w,t} \le P_{w,\max} \tag{4}$$

$$P_{w,t}^{l} \le P_{w,t} \le P_{w,t}^{u} \tag{5}$$

$$P_{w,t}^{l} = \mu^{w,t} - 1.96\sigma^{w,t} \tag{6}$$

$$P_{w,t}^{u} = \mu^{w,t} + 1.96\sigma^{w,t} \tag{7}$$

where, $P_{w,t}^{u}$ and $P_{w,t}^{l}$ are the upper and lower limits of wind farm w predicted output at time t, $\mu^{w,t}$ and $\sigma^{w,t}$ are the mean and standard deviation of probability distribution of the wind farm w predicted output at time t.

Too large range of wind power interval reduces economics and even makes the scheduling problem unsolvable. Therefore, the interval of wind power output is set as $\left[\mu^{w,t} - 1.96\sigma^{w,t}, \mu^{w,t} + 1.96\sigma^{w,t}\right]$ to ensure that at least 95% of the wind power output will be utilized [25].

2) SOLAR POWER CONSTRAINTS

Similar with the modelling of wind power constraints, solar power generation output also has upper and lower limits, which are expressed as follows:

$$0 \le P_{v,t} \le P_{v,\max} \tag{8}$$

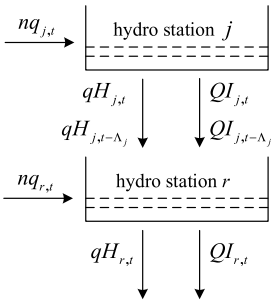

FIGURE 1. Hydraulic connection of cascade hydro stations.

$$P^{l}_{v,t} \le P_{v,t} \le P^{u}_{v,t} \tag{9}$$

$$P^{l}_{v,t} = \mu^{v,t} - 1.96\sigma^{v,t} \tag{10}$$

$$P^{u}_{v,t} = \mu^{v,t} + 1.96\sigma^{v,t} \tag{11}$$

where, $P^{u}_{v,t}$ and $P^{l}_{v,t}$ are the upper and lower limits of solar power station v predicted output at time t, $\mu^{v,t}$ and $\sigma^{v,t}$ are the mean and standard deviation of probability distribution of solar power station v predicted output at time t. In order to ensure that at least 95% of the solar power output can be utilized, the interval is set as $\left[\mu^{v,t} - 1.96\sigma^{v,t}, \mu^{v,t} + 1.96\sigma^{v,t}\right]$.

3) CASCADE HYDROPOWER CONSTRAINTS

Cascade hydro stations can not only meet the load demand of the power grid and ensure the safety of flood control in upstream and downstream areas, but also coordinate the relationship between water head, water inflow and output of hydro stations to improve the utilization rate [26]. Hydraulic connections between cascade hydro stations are shown in FIGURE 1.

There are not only hydraulic connections but also complicated electric connections among cascade hydro stations, which are expressed as follows:

a: HYDROPOWER OUTPUT CONSTRAINTS

$$P_{h,t} = \eta_h \cdot qH_{h,t} \cdot h_{h,t} \tag{12}$$

$$I_{h,t}P_{h,\min} \le P_{h,t} \le I_{h,t}P_{h,\max} \tag{13}$$

The hydropower output represented by (12) is a nonlinear function of water head and water consumption. In this paper, the mixed integer linearization method given in reference [27] is used to linearize it, as shown in Appendix.

b: WATER DISCHARGE CONSTRAINT

$$I_{h,t} \cdot qH_{h,\min} \le qH_{h,t} \le I_{h,t} \cdot qH_{h,\max} \tag{14}$$

c: WATER BALANCE CONSTRAINT

$$V_{h,t} = V_{h,t-1} + nq_{h,t} - qH_{h,t} - QI_{h,t} + \sum_{j \in U_h} \left(qH_{j,t-\Lambda_j} + QI_{j,t-\Lambda_j}\right) \tag{15}$$

d: RESERVOIR STORAGE CONSTRAINT

$$V_{h,\min} \le V_{h,t} \le V_{h,\max} \tag{16}$$

where, $V_{h,\max}$ and $V_{h,\min}$ are not the physical upper and lower limits of storage capacity, but the maximum and minimum storage capacity of each period considering irrigation, shipping and other factors.

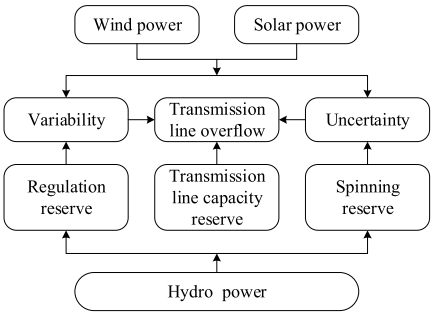

FIGURE 2. Structure of system reserve.

4) SYSTEM CONSTRAINTS

In the optimal scheduling model for wind-solar-hydro hybrid generation system, there are not only system power balance constraint and transmission constraints, but also reserve constraints due to the variability and uncertainty of wind and solar power, as shown in FIGURE 2.

System constraints formulations are as follows.

a: POWER BALANCE CONSTRAINT

$$\sum_{d=1}^{ND} PL_{d,t} = \sum_{w=1}^{NW} P_{w,t} + \sum_{v=1}^{NV} P_{v,t} + \sum_{h=1}^{NH} P_{h,t} \tag{17}$$

b: TRANSMISSION CONSTRAINTS

$$-TL_l \le \sum_{w=1}^{NW} D_{w,l}P_{w,t} + \sum_{v=1}^{NV} D_{v,l}P_{v,t} + \sum_{h=1}^{NH} D_{h,l}\left(P_{h,t} + I_{h,t}Ru_h + US_{h,t}\right) - \sum_{d=1}^{ND} D_{d,l}PL_{d,t} \le TL_l \tag{18}$$

$$-TL_l \le \sum_{w=1}^{NW} D_{w,l}P_{w,t} + \sum_{v=1}^{NV} D_{v,l}P_{v,t} + \sum_{h=1}^{NH} D_{h,l}\left(P_{h,t} - I_{h,t}Rd_h - DS_{h,t}\right) - \sum_{d=1}^{ND} D_{d,l}PL_{d,t} \le TL_l \tag{19}$$

c: REGULATION RESERVE CONSTRAINTS

The variability of wind power and solar power corresponds to the sudden change of wind speed and solar radiation, which is generally a fluctuating component with a period of 10s to 3min [28]. By employing a certain amount of regulation reserve from hydro stations, the hydropower can quickly adjust its output to cope with the variability of wind power and solar power. In other words, when a certain amount of regulation reserve from hydropower is employed,

the hydropower units can automatically track the scheduled output curve and keep the power output of wind-solar-hydro hybrid generation system equal to the scheduled value.

$$\sum_{h=1}^{NH} I_{h,t} Ru_h \geq \alpha \left(P^u_{w,t} - P_{w,t}\right) + \beta \left(P^u_{v,t} - P_{v,t}\right) \tag{20}$$

$$\sum_{h=1}^{NH} I_{h,t} Rd_h \geq \alpha \left(P_{w,t} - P^l_{w,t}\right) + \beta \left(P_{v,t} - P^l_{v,t}\right) \tag{21}$$

The uncertainty in the output of wind and solar power (α, β) are with a typical error in the range of 15% to 25% [29].

d: SPINNING RESERVE CONSTRAINTS

In wind-solar-hydro hybrid generation systems, the predictions of wind power and solar power are more difficult than the load predictions. The uncertainty of wind power and solar power corresponds to hourly prediction error, and the scheduling of spinning reserve will be needed to maintain an adequate level of supply reliability [30]. If the prediction values of wind power and solar power are higher than actual values, the hydropower need to rapidly increase to make up the gap between predicted value and actual value, and the system needs to provide up spinning reserve. On the contrary, if the prediction values of wind power and solar power are lower than actual values, the hydropower need to rapidly decrease to balance the surplus, and the system needs to provide down spinning reserve.

The up-spinning reserve capacity constraints are expressed as:

$$US_{h,\max} = \tau_u P_{h,\max} \tag{22}$$

$$\sum_{h=1}^{NH} US_{h,t} \geq \lambda^+ \cdot P_{w,t} + \mu^+ \cdot P_{v,t} \tag{23}$$

$$US_{h,t} \leq \min\left\{US_{h,\max}, I_{h,t}\left(P_{h,\max} - P_{h,t} - Ru_h\right)\right\} \tag{24}$$

The down spinning reserve capacity constraints are expressed as:

$$DS_{h,\max} = \tau_d P_{h,\max} \tag{25}$$

$$\sum_{h=1}^{NH} DS_{h,t} \geq \lambda^- \cdot P_{w,t} + \mu^- \cdot P_{v,t} \tag{26}$$

$$DS_{h,t} \leq \min\left\{DS_{h,\max}, I_{h,t}\left(P_{h,t} - P_{h,\min} - Rd_h\right)\right\} \tag{27}$$

The maximum up (or down) spinning reserve of any single hydro station (τ_u, τ_d) could not contribute more than 20% of its related capacity. The up (or down) spinning reserve requirements for wind and solar power ($\lambda^{\pm}$, $\mu^{\pm}$) account for about 20% of their actual output [21].

The above scheduling model is built on the assumption that the cascade hydro power is bundled with wind power and solar power. Notice that, for example, in the wind-solar-cascade hydro hybrid Generation system of Yalong River, which located in Sichuan Province of China, the stakeholders of the power stations (plants) are the same one, i.e., Yalong River Hydropower Development Company LTD, Chengdu, China, which makes the assumption reasonable. However, commonly, the stakeholders of the power stations (plants) are not the same one. Then, to ensure joint operation of wind-PV-hydro complementary generation system owned by multiple stakeholders, incentive methods should be employed to allocate incremental benefit from joint operation of multi-stakeholders [31].

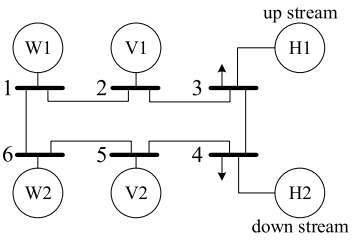

FIGURE 3. System diagram for case A.

To relief computation burden, the Benders decomposition is utilized to divide this model into a master problem and a transmission checking subproblem. The objective of master problem is (3). It is subject to (4)-(17), (20)-(27) and the Benders cuts generated from the subproblem (18)-(19). Details about Benders decomposition can be found in [25].

III. SIMULATION RESULT

Commercial computing software has a good performance in solving optimization problems with multi-variables, multi periods and nonlinear constraints. Among them, CPLEX has evolved into an effective optimization tool for linear programming, mixed integer programming and quadratic programming, which can provide excellent solutions for complex mixed integer linear programming problems. The nonlinear factors are linearized on the premise of meeting the accuracy requirements as described in the appendix, and then solved by MILP solver (branch-and-bound algorithm) in CPLEX. In this paper, the simulations are solved with CPLEX12.6 on a personal DELL computer with an Intel 2.6 GHz dual core processor and 6 GB of RAM.

A. CASE A

To verify the effectiveness of the proposed model, we firstly conduct a simulation analysis on the hybrid generation system consisting of two wind farms, two solar power stations and a cascade hydropower station (composed of two hydro stations) over one day, with 24 periods in total. System structure is shown in FIGURE 3.

Due to the influence of natural inflow on hydropower output and energy storage, we implement simulations for two typical scenarios, namely dry season and wet season. System load of one day in the wet season is shown in FIGURE 4, and approximately 40% more than that in the dry season. Parameters of hydropower units are shown in Table 1. Transmission line limits are shown in Table 2. The hydropower output function is piecewise linearized into 9*9 grids. We obtain the wind and solar power data from the dataset of National Renewable Energy Laboratory (NREL) (https://www.nrel.gov/electricity/transmission.html).

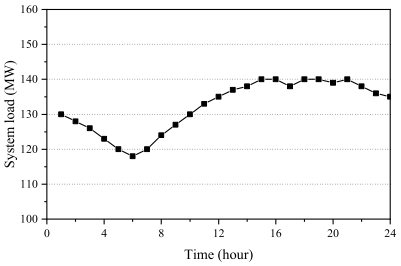

FIGURE 4. System total load demand.

TABLE 1. Parameters of hydropower units.

Unit		1	2
Λ_h	(h)	2	0
$P_{h,\min}$	(MW)	10	10
$P_{h,\max}$	(MW)	180	160
$qH_{h,\min}$	($10^4 m^3$)	20	20
$qH_{h,\max}$	($10^4 m^3$)	150	180
$V_{h,\min}$	($10^4 m^3$)	200	200
$V_{h,\max}$	($10^4 m^3$)	1000	1200
V_h^{ini} (wet)	($10^4 m^3$)	500	500
V_h^{ini} (dry)	($10^4 m^3$)	300	300
$Rd_h\left(Ru_h\right)$	(MW)	4	8

TABLE 2. Transmission line data.

From Bus	To Bus	Transmission limit (MW)
1	2	60
1	6	50
2	3	75
3	4	80
4	5	80
5	6	50

The output of the hybrid generation system in wet season and dry season are shown in FIGURE 5 and FIGURE 6 respectively.

As shown in FIGURE 5(a) and FIGURE 6(a), when the regulation reserve and spinning reserve are not taken into account, the output power of hydropower is zero among 12h-17h, i.e. the hydro stations are off, so they cannot provide down regulation reserve and down spinning reserve to smooth the fluctuation of wind and solar power. However, in the hybrid generation system including spinning reserve and regulation reserve, as shown in FIGURE 5(b) and FIGURE 6(b), the hydro stations are in working state in each time period with sufficient ability to ensure the safe operation of the system.

From FIGURE 5(b) and FIGURE 6(b), we can see that the total output of wind and solar power gradually increases at 7h until reaching peak at 18h. During these periods, hydro stations store water as much as possible and keep output at a minimum value to provide reserve. When the output of solar power is zero at night, hydropower increases output to ensure meeting load demand.

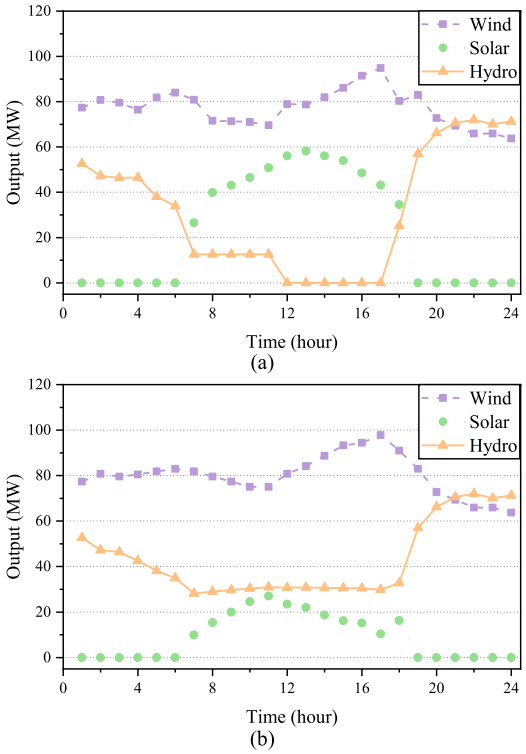

FIGURE 5. Output in wet season (a) Excluding spinning reserve and regulation reserve (b) Including spinning reserve and regulation reserve.

TABLE 3. Objective values.

Season	Reserve	Abandoned wind and solar power/MWh	Abandoned hydropower /MWh	Hydropower storage /MWh
Wet	Excluding	69.3	1532	700
	Including	351.7	1282	700
Dry	Excluding	73.5	0	291
	Including	265	0	139

From Table 3, we can see that in the wet season, the output of hydropower increases to provide reserve, and the abandoned hydropower decreases accordingly. At the same time, wind and solar power reduce output to ensure the balance of supply and demand, thus the abandoned wind and solar power increase. Due to the abundant natural inflow, the hydropower storage reaches the maximum value at the end of the dispatching periods. However, in the dry season, due to the lack of natural inflow, there is no abandoned hydropower after power generation, and the hydropower storage is far lower than that in the wet season. After using the scarce water inflow to provide reserve, the hydropower storage is also reduced.

According to the optimal scheduling model, the regulation reserve demand and regulation reserve capability can be defined as follows:

$$RD_t = \alpha\left(P_{w,t}^u - P_{w,t}^l\right) + \beta\left(P_{v,t}^u - P_{v,t}^l\right) \quad (28)$$

$$RC_t = \sum_{h=1}^{NH} I_{h,t} Ru_h \left(Rd_h\right) \quad (29)$$

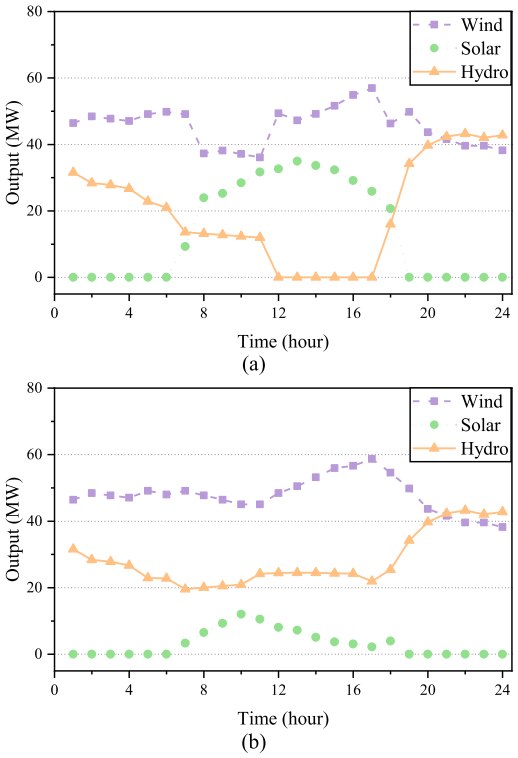

FIGURE 6. Output in dry season (a) Excluding spinning reserve and regulation reserve (b) Including spinning reserve and regulation reserve.

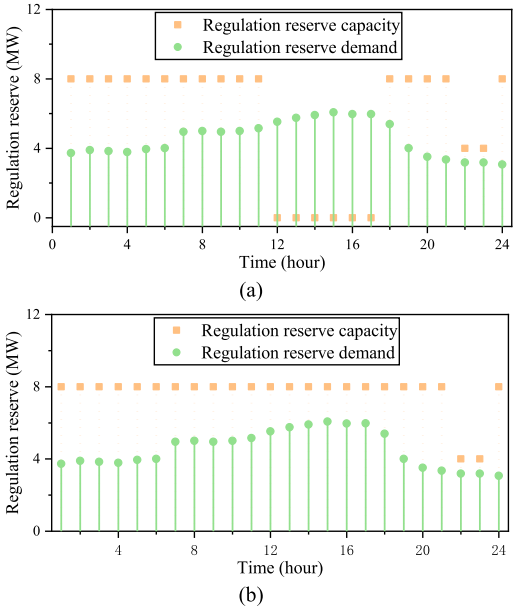

FIGURE 7. Regulation reserve demand and capacity in wet season (a) Excluding regulation reserve (b) Including regulation reserve.

To verify the necessity of regulation reserve, simulation results of the proposed model are shown in FIGURE 7 and FIGURE 8.

From FIGURE 7(b) and FIGURE 8(b), when regulation reserve is included, the regulation reserve capacity can meet the reserve demand in the 24 scheduling periods. In the dry season, despite the lack of natural inflow, the regulation reserve capacity provided by hydropower is relatively low

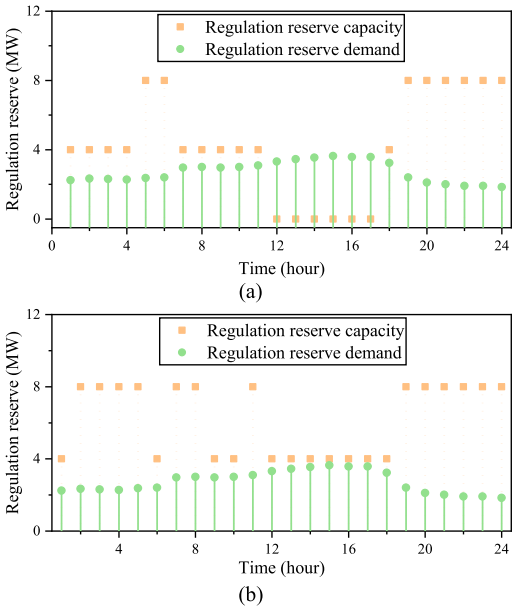

FIGURE 8. Regulation reserve demand and capacity in dry season (a) Excluding regulation reserve (b) Including regulation reserve.

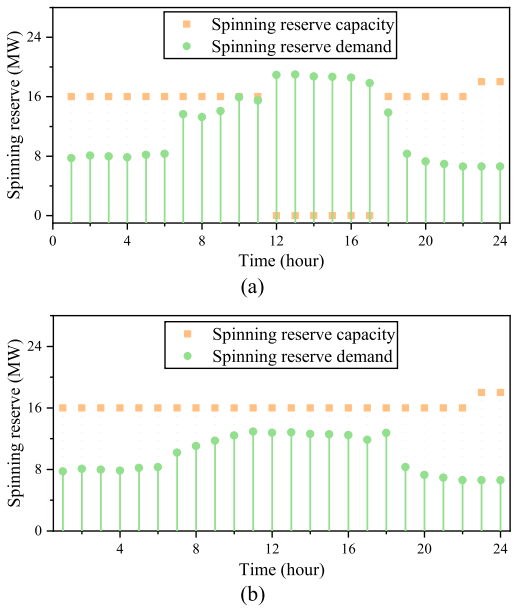

FIGURE 9. Spinning reserve demand and capacity in wet season (a) Excluding spinning reserve (b) Including spinning reserve.

during 12h−18h, it can also meet the reserve demand for the wind and solar power variations. However, when regulation reserve is excluded, as shown in FIGURE 7(a) and FIGURE 8(a). it is shown that no matter in the wet season or in the dry season, the optimal scheduling model reserve can't meet the regulation demand during 12h−17h, therefore the scheduling results excluding regulation reserve cannot provide enough down regulation capacity to cope with the wind and solar power output uncertainty.

According to the optimal scheduling model, the spinning reserve demand is defined as:

$$BD_t = \lambda \cdot P_{w,t} + \mu \cdot P_{v,t} \tag{30}$$

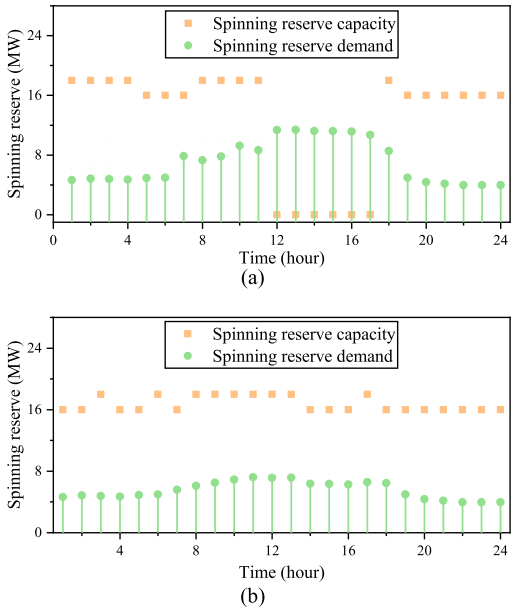

FIGURE 10. Spinning reserve demand and capacity in dry season (a) Excluding spinning reserve (b) Including spinning reserve.

To verify the necessity of considering spinning reserve, the simulation results for spinning reserve demand and capacity under the optimal scheduling model are shown in FIGURE 9 and FIGURE 10.

We can see that both in the wet season and dry season, the optimal scheduling model for wind-solar-hydro hybrid generation system excluding spinning reserve constraints lacks adequate capacity to meet the spinning reserve demand during 12h−17h. As shown in FIGURE 9(a) and FIGURE 10(a), the hydropower in corresponding periods has no output during 12h−17h, therefore the fluctuations of wind and solar power output cannot be accommodated in these periods. As a result, the scheduling scheme is not feasible. However, when spinning reserve constraints are considered, as shown in FIGURE 9(b) and FIGURE 10(b), the generation system has enough spinning reserve capacity in each scheduling period both in the wet season and dry season.

We set different spinning reserve requirement coefficients to test the influences on the performance of the proposed scheduling model. In order to facilitate the analysis, we set the requirement coefficients of wind power and solar power to be equal, i.e., $\lambda = \mu$. Results show that the system has adequate capacity to meet both up and down spinning reserve demand, and the change of objective function values is shown in FIGURE 11.

It can be seen from FIGURE 11(a) that due to the sufficient inflow in wet season, the hydropower storage is still at the maximum value. Hydropower increases output to provide sufficient reserve capacity to meet growing reserve demand, while wind and solar power reduce output to meet power balance. Therefore, the hybrid system abandons less hydropower but more wind and solar power. As shown in FIGURE 11(b), as more hydropower is used to provide spinning reserve, the hydropower storage is greatly reduced in dry season.

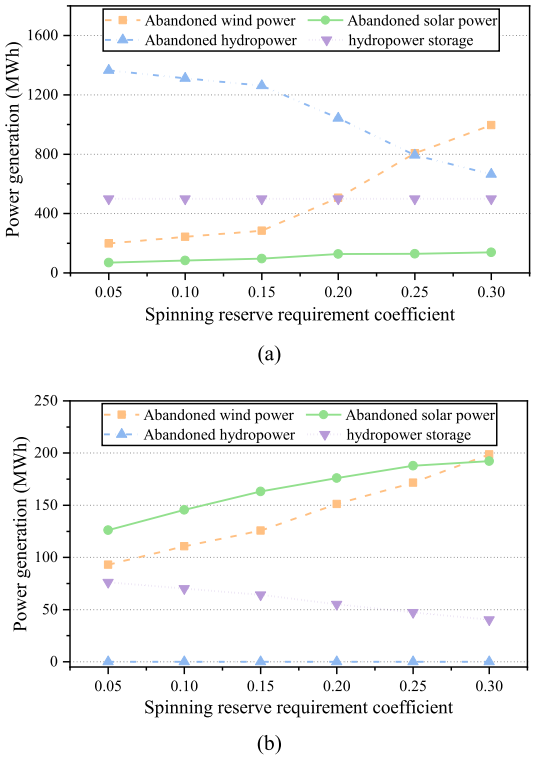

FIGURE 11. Abandoned power and stored hydropower under different spinning reserve requirements (a) Wet season (b) Dry season.

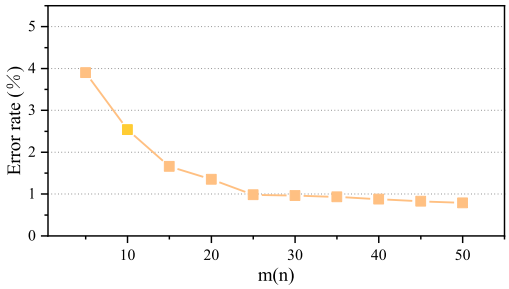

FIGURE 12. Solution accuracy for different subintervals.

Error rate is an important index to judge the solution accuracy, which reflects the gap to the most accurate results. The variation of error rate and computation time with the number of subintervals for (12) are shown in FIGURE 12 and FIGURE 13. For the sake of analysis, we assume that qH and v are equally divided, i.e., m = n.

From FIGURE 12 and FIGURE 13, we can see that more subintervals can lead to a more accurate solution and longer computation time. When the number of segments is greater than or equal to 30 ($m \geq 30$), the accuracy improves by a very small margin. Therefore, appropriate number of segments should be selected to achieve good accuracy and save much more computation time.

B. CASE B

With the rapid development of clean energy power generation technology, in China, the development of wind, solar, hydro and other clean energy bases is expanding.

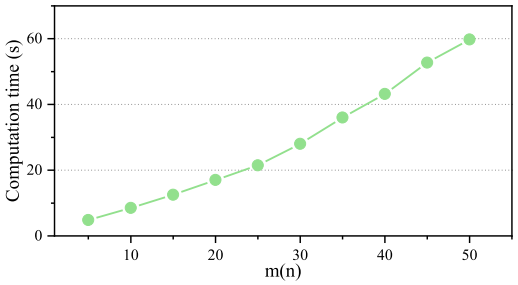

FIGURE 13. Computation time for different subintervals.

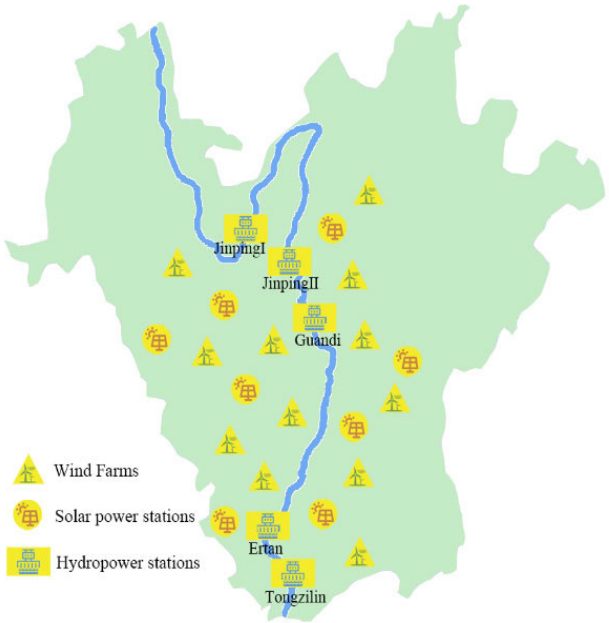

FIGURE 14. Topographic map of lower Yalong River basin.

TABLE 4. Parameters of the hydro stations.

Hydro station	$P_{h,\min}$ /MW	$P_{h,\max}$ / MW	$qH_{h,\min}$ /10^4m^3	$qH_{h,\max}$ /10^4m^3	$V_{h,\min}$ /10^4m^3	$V_{h,\max}$ /10^4m^3
Jinping I	1086	3000	150	2058	285000	776000
Jinping II	1972	4200	145	1784	921	1401
Guandi	709.8	1800	145	2344	73160	76000
Ertan	1000	2750	145	2226	243000	580000
Tong zilin	171	450	160	3473.2	7664	9120

By June 2019, the total installed capacity of clean energy such as hydropower, wind power and solar power in China has reached 6.8×10^{10}KW, accounting for 37.2% of the total installed generation capacity in China.

Yalong River, located in Sichuan Province of China, flows through three administrative regions, with a total length of 1571km, a total drainage area of about 1.36×10^5km^2, and an annual runoff of about 600km^3. It is rich in wind, solar and hydropower resources which makes it become a typical representative base of wind-solar-hydro hybrid generation system with cascade hydropower. At present, 23 cascade hydro stations with a total installed capacity of 28.85 million kW and an annual hydropower generation of 133.3 billion kWh have been planned along the Yalong River. The total planned capacity of wind and solar power is 3.0689×10^7kW, including 17 wind farms and 3 solar power stations.

TABLE 5. Optimization results of case B.

Scenario	Iteration	Objective solution /MWh	Final gap /%
①	579824	-55889	2.76
②	580452	-55268	3.81
③	594025	-20605	2.93
④	520017	-14026	2.85

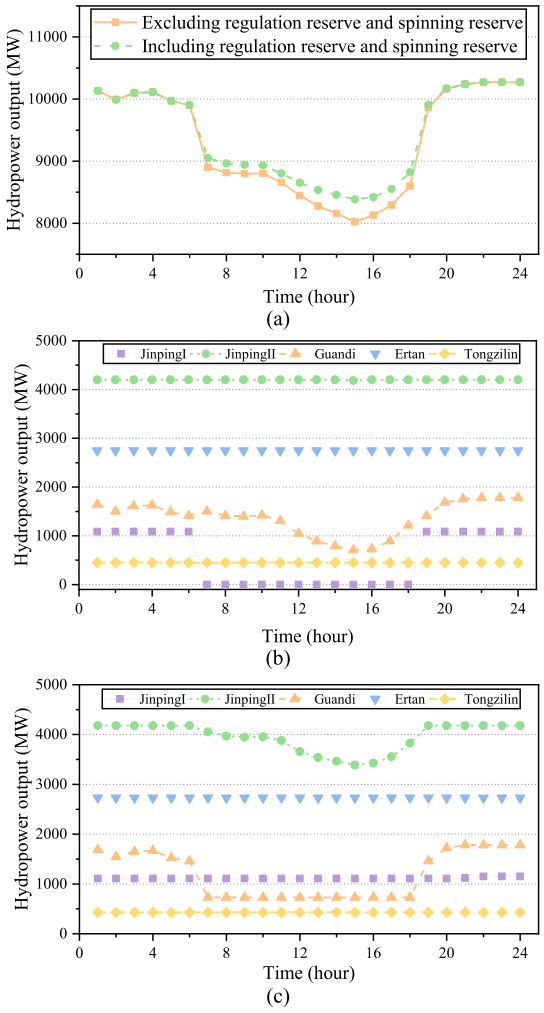

FIGURE 15. Hydropower output in wet season (a) Total hydropower output (b) Excluding regulation reserve and spinning reserve (c) Including regulation reserve and spinning reserve.

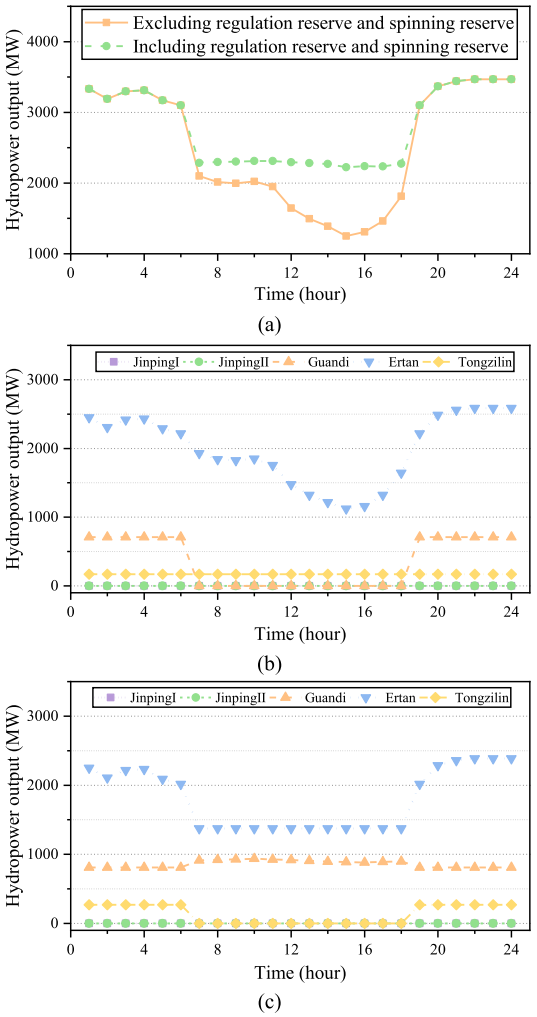

FIGURE 16. Hydropower output in dry season (a) Total hydropower output (b) Excluding regulation reserve and spinning reserve (c) Including regulation reserve and spinning reserve.

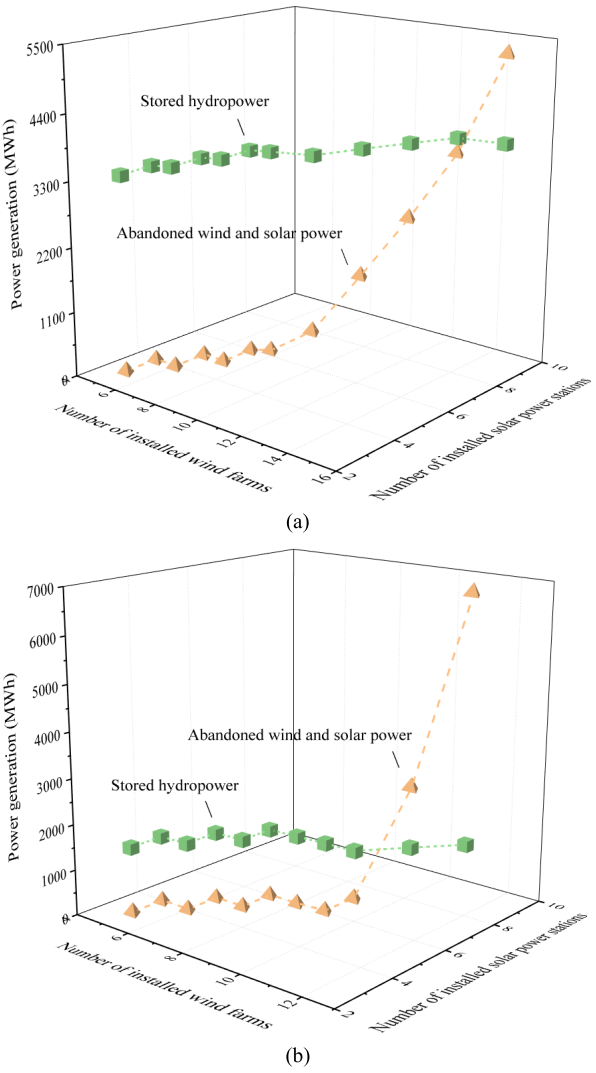

FIGURE 17. Abandoned wind and solar power and stored hydropower under various installations (a) Wet season (b) Dry season.

A case study is given in this section to test the application of the presented model in the lower Yalong River basin. The test system consists of 12 wind power stations, 8 solar power stations and 5 hydro stations. Topographic map of the study area is shown in FIGURE 14, and the main parameters are given in Table 4. When spinning reserve and regulation reserve constraints are considered in the problem, the model has 15135 variables, including 3568 binary variables and 4792 constraints.

We consider four scenarios: ① Excluding regulation reserve and spinning reserve in wet season; ② Including regulation reserve and spinning reserve in wet season; ③ Excluding regulation reserve and spinning reserve in dry season; ④ Including regulation reserve and spinning reserve in dry season. We set a time limit of 15min as the stopping criterion because the operators should make a quick decision in practice. The optimization results obtained from the four scenarios are shown in Table 5, where the final gap is expressed as

$$\frac{objective\ solution - lower\ objective}{lower\ objective\ bound} \times 100\%$$

The optimized objective function values are −55889MWh, −55268MWh, −20605MWh and −14026MWh, respectively. The narrowest final gap is 2.76% in Scenario ①, while the widest final gap is 3.81% in Scenario ②. The results are quite acceptable because of the large number of variables in this problem. Furthermore, it is worth noting in particular that the final gap means the objective solution is at least within the percentage of the global optimal solution; the longer run may only tighten the bounds but not improve the objective solution [26].

It can be seen from FIGURE 15(a) and FIGURE 16(a) that during 7h − 18h, hydropower increases output to meet the regulation reserve and spinning reserve demand when including regulation reserve and spinning reserve. Since the storage capacity of Guandi is 6 times that of JinpingII and JinpingI, Guandi reduces output to store energy in the wet season, as shown in FIGURE 15(b). However, due to the shortage of natural inflow in the dry season, the upstream hydro stations (JinpingI and JinpingII) are off to accumulate more energy

storage, and Guandi and Ertan reduce output to meet the load demand, as shown in FIGURE 16(b). When considering regulation reserve and spinning reserve, the upstream hydro stations can consume less water to provide reserve. Therefore, during the wet season, JinpingI increases output for reserve, and JinpingII and Guandi reduce output to keep output-load balance, as shown in FIGURE 15(c). In the dry season, Guandi provides regulation reserve capacity and spinning reserve capacity, and Ertan and Tongzilin reduce output, as shown in FIGURE 16(c).

FIGURE 17 shows values of the abandoned wind and solar power and the hydropower storage under different installed conditions of wind farms and solar power stations. We assume that the installed capacity of each wind farm and solar power station is the same, both of which are 200MW.

As can be seen from FIGURE 17, the larger the installed capacity of wind and solar power are, the larger the hydropower storage is, but also the larger the abandoned wind and solar power are. The growth rate of the abandoned power is much higher than that of hydropower storage when the installed wind farms and solar power stations exceeds 15, which is against the goal of conserving resources, suggesting that the system can no longer install wind farms and solar power stations. Such numerical results give an indicator to provide valuable information for installation of wind farms and solar power stations for a given cascade hydropower scenario.

IV. CONCLUSION

In this paper, we develop a short-term optimal scheduling model for wind-solar-hydro hybrid power generation system with cascade hydropower, in which hydropower provide spinning reserve and regulation reserve, so as to save resources on the premise of ensuring the safe and stable operation of the system. After linearizing the nonlinear constraints, we use MILP to solve the complex scheduling problem. In the case studies, we demonstrate that the spinning reserve and regulation reserve are vital to maintain an adequate level of supply reliability and security due to the integration of wind and solar power. Moreover, the proposed model can provide valuable information for installation of wind farms and solar power stations.

Generally, hydropower units have certain vibration areas, and the units cannot operate continuously for a long time in the prohibited operating zones (POZs). The POZs of hydropower units have not considered in the presented scheduling model, which should be addressed in the near future. Furthermore, scheduling models of different time scales for hybrid generation systems should be studied, and the more prominent prediction error in wind and solar power prediction in long time scales should be considered.

APPENDIX

The hydropower production is determined by the water consumption and the water head. Within the allowable range of error, the water head can be approximated as a unitary function of reservoir storage:

$$h_{h,t} = h_{h,0} + \mu_h \cdot V_{h,t} \tag{A-1}$$

where, $h_{h,0}$ is the constant coefficient of reservoir, μ_h is the reservoir storage capacity coefficient.

Then power generation is the nonlinear binary function of water consumption and reservoir storage, which can be expressed as:

$$P_{h,t} = \eta_h \cdot qH_{h,t} \cdot \left(h_{h,0} + \mu_h \cdot V_{h,t}\right) \tag{A-2}$$

For the sake of discussion, we rewrite (A-2) as follows by ignoring subscripts:

$$P = \eta \cdot qH \cdot (h_0 + \mu \cdot V) \tag{A-3}$$

qH and V can be divided into subintervals $[q_k, q_{k+1}]$ and $[v_l, v_{l+1}]$, where $k = 1 \cdots m-1$, $l = 1 \cdots n-1$. Thus, the original function is divided into a grid of $(m-1)\cdot(n-1)$, and each point corresponds to $P_{k,l} = \eta \cdot q_k \cdot [h_0 + \mu \cdot V_l]$ in the original function. Each grid element is divided into two triangles, i.e., the upper left corner and the lower right corner. $\varsigma_{k,l}$ and $\zeta_{k,l}$ are indexes representing the location in the two triangles. Therefore, the hydropower output function can be piecewise linearized as follows [27]:

$$\begin{cases} q = \sum_{k=1}^{m}\sum_{l=1}^{n} q_k \cdot \phi_{k,l} \quad V = \sum_{k=1}^{m}\sum_{l=1}^{n} V_l \cdot \phi_{k,l} \\ \sum_{k=1}^{m}\sum_{l=1}^{n} \phi_{k,l} = 1 \quad \sum_{k=1}^{m}\sum_{l=1}^{n} \left(\varsigma_{k,l} + \zeta_{k,l}\right) = 1 \\ \phi_{k,l} \geq 0 \quad \varsigma_{k,l}, \zeta_{k,l} \in 0, 1 \quad P = \sum_{k=1}^{m}\sum_{l=1}^{n} P_{k,l} \cdot \phi_{k,l} \\ \phi_{k,l} \leq \varsigma_{k,l-1} + \varsigma_{k,l} + \varsigma_{k,l+1} + \zeta_{k-1,l} + \zeta_{k,l} + \zeta_{k+1,l} \end{cases} \tag{A-4}$$

Thus, the hydropower output function (12) is transformed from a non-linear function to a piecewise linear function (A-4) composed of continuous variables, integer variables and binary variables.

REFERENCES

[1] G. Papaefthymiou and K. Dragoon, "Towards 100% renewable energy systems: Uncapping power system flexibility," *Energy Policy*, vol. 92, pp. 69–82, May 2016.

[2] M. Basu, "Combined heat and power dynamic economic dispatch with demand side management incorporating renewable energy sources and pumped hydro energy storage," *IET Gener., Transmiss. Distrib.*, vol. 13, no. 17, pp. 3771–3781, Sep. 2019.

[3] X. Zhang, G. Ma, W. Huang, S. Chen, and S. Zhang, "Short-term optimal operation of a wind-pv-hydro complementary installation: Yalong River, Sichuan Province, China," *Energies*, vol. 11, no. 868, pp. 1–19, Apr. 2018.

[4] X. Ge, Y. Jin, Y. Fu, Y. Ma, and S. Xia, "Multiple-cut benders decomposition for wind-hydro-thermal optimal scheduling with quantifying of various types of reserves," *IEEE Trans. Sustain. Energy*, vol. 11, no. 3, pp. 1358–1369, Jul. 2019.

[5] J. Shi, W.-J. Lee, and X. Liu, "Generation scheduling optimization of wind-energy storage system based on wind power output fluctuation features," *IEEE Trans. Ind. Appl.*, vol. 54, no. 1, pp. 10–17, Jan. 2018.

[6] J. Li, S. Wang, L. Ye, and J. Fang, "A coordinated dispatch method with pumped-storage and battery-storage for compensating the variation of wind power," *Protection Control Mod. Power Syst.*, vol. 3, no. 1, pp. 21–34, Dec. 2018.

[7] S. Xia, Z. Ding, T. Du, D. Zhang, M. Shahidehpour, and T. Ding, "Multi-time scale coordinated scheduling for the combined system of wind power, photovoltaic, thermal generator, hydro pumped storage, and batteries," *IEEE Trans. Ind. Appl.*, vol. 56, no. 3, pp. 2227–2237, May 2020.
[8] L. V. L. Abreu, M. E. Khodayar, M. Shahidehpour, and L. Wu, "Risk-constrained coordination of cascaded hydro units with variable wind power generation," *IEEE Trans. Sustain. Energy*, vol. 3, no. 3, pp. 359–368, Jul. 2012.
[9] Y. Liu, S. Tan, and C. Jiang, "Interval optimal scheduling of hydro-PV-wind hybrid system considering firm generation coordination," *IET Renew. Power Gener.*, vol. 11, no. 1, pp. 63–72, Jan. 2017.
[10] Y. An, Z. Zhao, S. Wang, Q. Huang, and X. Xie, "Coordinative optimization of hydro-photovoltaic-wind-battery complementary power stations," *CSEE J. Power Energ. Syst.*, vol. 6, no. 2, pp. 410–418, Jun. 2020.
[11] J. Matevosyan, M. Olsson, and L. Söder, "Hydropower planning coordinated with wind power in areas with congestion problems for trading on the spot and the regulating market," *Electr. Power Syst. Res.*, vol. 79, no. 1, pp. 39–48, Jan. 2009.
[12] D. Apostolopoulou and M. McCulloch, "Optimal short-term operation of a cascaded hydro-solar hybrid system: A case study in kenya," *IEEE Trans. Sustain. Energy*, vol. 10, no. 4, pp. 1878–1889, Oct. 2019.
[13] J.-J. Shen, Q.-Q. Shen, S. Wang, J.-Y. Lu, and Q.-X. Meng, "Generation scheduling of a hydrothermal system considering multiple provincial peak-shaving demands," *IEEE Access*, vol. 7, pp. 46225–46239, 2019.
[14] H. Zhang, Z. Lu, W. Hu, Y. Wang, L. Dong, and J. Zhang, "Coordinated optimal operation of hydro–wind–solar integrated systems," *Appl. Energy*, vol. 242, pp. 883–896, May 2019.
[15] S. Hagspiel, A. Papaemannouil, M. Schmid, and G. Andersson, "Copula-based modeling of stochastic wind power in europe and implications for the Swiss power grid," *Appl. Energy*, vol. 96, pp. 33–44, Aug. 2012.
[16] J. Munkhammar, J. Widén, and L. M. Hinkelman, "A copula method for simulating correlated instantaneous solar irradiance in spatial networks," *Sol. Energy*, vol. 143, pp. 10–21, Feb. 2017.
[17] D. Yang, Z. Dong, T. Reindl, P. Jirutitijaroen, and W. M. Walsh, "Solar irradiance forecasting using spatio-temporal empirical kriging and vector autoregressive models with parameter shrinkage," *Sol. Energy*, vol. 60, no. 1, pp. 235–245, Dec. 2013.
[18] C.-L. Chen, "Optimal wind–thermal generating unit commitment," *IEEE Trans. Energy Convers.*, vol. 23, no. 1, pp. 273–280, Mar. 2008.
[19] G. Morales-Espana, R. Baldick, J. Garcia-Gonzalez, and A. Ramos, "Power-capacity and ramp-capability reserves for wind integration in power-based UC," *IEEE Trans. Sustain. Energy*, vol. 7, no. 2, pp. 614–624, Apr. 2016.
[20] B. Liu, J. R. Lund, S. Liao, X. Jin, L. Liu, and C. Cheng, "Peak shaving model for coordinated Hydro-Wind-Solar system serving local and multiple receiving power grids via HVDC transmission lines," *IEEE Access*, vol. 8, pp. 60689–60703, Apr. 2020.
[21] Y. Li, T. Zhao, C. Liu, Y. Zhao, Z. Yu, K. Li, and L. Wu, "Day-ahead coordinated scheduling of hydro and wind power generation system considering uncertainties," *IEEE Trans. Ind. Appl.*, vol. 55, no. 3, pp. 2368–2377, May 2019.
[22] C. Peng, P. Xie, L. Pan, and R. Yu, "Flexible robust optimization dispatch for hybrid wind/photovoltaic/hydro/thermal power system," *IEEE Trans. Smart Grid*, vol. 7, no. 2, pp. 751–762, Mar. 2016.
[23] J. Shen, C. Cheng, R. Cao, Q. Shen, X. Li, Y. Wu, and B. Zhou, "Generation scheduling of a hydrodominated provincial system considering forecast errors of wind and solar power," *J. Water Resour. Planning Manage.*, vol. 145, no. 10, Oct. 2019, Art. no. 04019043.
[24] R. Zhong, C. Cheng, S. Liao, and Z. Zhao, "Short-term scheduling of expected output-sensitive cascaded hydro systems considering the provision of reserve services," *Energies*, vol. 13, no. 10, pp. 1–15, 2020.
[25] B. Zhou, G. Geng, and Q. Jiang, "Hydro-thermal-wind coordination_newline in day-ahead unit commitment," *IEEE Trans. Power Syst.*, vol. 31, no. 6, pp. 4626–4637, Nov. 2016.
[26] X. Li, T. Li, J. Wei, G. Wang, and W. W.-G. Yeh, "Hydro unit commitment via mixed integer linear programming: A case study of the three gorges project, China," *IEEE Trans. Power Syst.*, vol. 29, no. 3, pp. 1232–1241, May 2014.
[27] L. Wu, M. Shahidehpour, and Z. Li, "GENCO's risk-constrained hydrothermal scheduling," *IEEE Trans. Power Syst.*, vol. 23, no. 4, pp. 1847–1858, Nov. 2008.
[28] Y. S. X. Xue Lei and F. Xue, "A review on impacts of wind power uncertainties on power systems," *Proc. CSEE*, vol. 34, no. 29, pp. 5029–5040, 2014.
[29] J. Garcia-Gonzalez, R. M. R. de la Muela, L. M. Santos, and A. M. Gonzalez, "Stochastic joint optimization of wind generation and pumped-storage units in an electricity market," *IEEE Trans. Power Syst.*, vol. 23, no. 2, pp. 460–468, May 2008.
[30] S. Xia, M. Zhou, and G. Li, "A coordinated active power and reserve dispatch approach for wind power integrated power systems considering line security verification," *Proc. CSEE*, vol. 33, no. 13, pp. 18–26, May 2013.
[31] E. Faria, L. A. Barroso, R. Kelman, S. Granville, and M. V. Pereira, "Allocation of firm-energy rights among hydro plants: An Aumann–Shapley approach," *IEEE Trans. Power Syst.*, vol. 24, no. 2, pp. 541–551, May 2009.

JUN XIE (Member, IEEE) received the B.Eng. and Ph.D. degrees from Hohai University, China, in 2002 and 2007, respectively, both in energy and electrical engineering. From 2007 to 2010, he was a Postdoctoral Fellow with the Department of Electrical Engineering, Zhejiang University, China, and the Department of Electrical and Electronic Engineering, The University of Hong Kong, China. He joined the faculty of Hohai University, in 2017, where he has been Professor since the same year. His research interests are engineering, economic and environmental issues in the electric power industry.

YIMIN ZHENG received the B.Eng. degree in energy and electrical engineering from the Nanjing University of Posts and Telecommunications, China, in 2018. She is currently pursuing the M.Eng. degree with the Department of Energy and Electrical Engineering, Hohai University, China. Her research interests include power system optimal operation and electricity market.

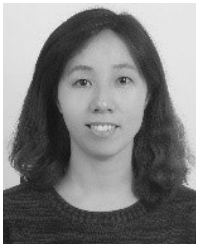

XUEPING PAN (Member, IEEE) received the B.Eng. and M.S. degrees in electrical engineering from Hohai University, Nanjing, China, in 1994 and 2000, respectively, and the Ph.D. degree from Zhejiang University, China, in 2008. From 2009 to 2010, she was a Visiting Scholar at Washington State University, Pullman, WA, USA. She is currently a Professor with the College of Energy and Electrical Engineering, Hohai University. Her research interests include modeling, analysis, and control of power system integrated with high portion renewable power generation.

YUAN ZHENG received the B.Eng., M.Eng., and Ph.D. degrees from Hohai University, China, in 1986, 1997, and 2004, respectively, all in hydropower engineering. He joined the faculty of Hohai University, in 1986, where he has been a Professor, since 2004. His current research interest is hydropower system modeling, control, and automation.

LIQIN ZHANG received the B.Eng. degree in electrical engineering from Nanjing Normal University, China, in 2018. She is currently pursuing the M.Eng. degree with Hohai University, China. Her current interest is the electricity market and power system economics.

YONGSHENG ZHAN received the B.Eng. degree in electrical engineering and automation from Harbin Engineering University, China, in 2003, and the M.Sc. degree in detection technology and automation equipment from Harbin Engineering University, in 2008. From 2003 to 2005, he was engaged in generator structure design at the Institute of Large Motor, Harbin Electric Machinery Factory Co., Ltd., China. He returned to Harbin Engineering University in 2005. Since 2008, he has been engaged in the optimization of power generation scheduling and dispatching at the Yalong River Hydropower Development Company, Sichuan, China.